Controlled Grafting of Polymer Brushes on Poly(vinylidene fluoride) Films by Surface-Initiated Atom Transfer Radical Polymerization

Dongmei Liu,[1] Yiwang Chen,[2,1] Ning Zhang,[1] Xiaohui He[2]

[1]*Department of Chemistry, Nanchang University, Nanchang 330047, People's Republic of China*
[2]*School of Materials Science and Engineering, Nanchang University, Nanchang 330047, People's Republic of China*

Received 5 August 2005; accepted 30 August 2005
DOI 10.1002/app.23066
Published online in Wiley InterScience (www.interscience.wiley.com).

ABSTRACT: Controlled grafting of well-defined polymer brushes on the poly(vinylidene fluoride) (PVDF) films was carried out by the surface-initiated atom transfer radical polymerization (ATRP). Surface-initiators were immobilized on the PVDF films by surface hydroxylation and esterification of the hydroxyl groups covalently linked to the surface with 2-bromoisobutyrate bromide. Homopolymer brushes of methyl methacrylate (MMA) and poly(ethylene glycol) monomethacrylate (PEGMA) were prepared by ATRP from the α-bromoester-functionalized PVDF surface. The chemical composition of the graft-functionalized PVDF surfaces was characterized by X-ray photoelectron spectroscopy (XPS) and attenuated total reflectance (ATR)–FTIR spectroscopy. Kinetics study revealed a linear increase in the graft concentration of PMMA and PEGMA with the reaction time, indicating that the chain growth from the surface was consistent with a "controlled" or "living" process. The "living" chain ends were used as the macroinitiator for the synthesis of diblock copolymer brushes. Water contact angles on PVDF films were reduced by surface grafting of PEGMA and MMA. © 2006 Wiley Periodicals, Inc. J Appl Polym Sci 101: 3704–3712, 2006

Key words: poly(vinylidene fluoride); ATRP; polymer brush; surface modification; living polymerization

INTRODUCTION

Surface modification of polymers via molecular design is one of the most versatile approaches to imparting new functionalities, such as improved hydrophilicity, biocompatibility, conductivity, and lubricative and adhesive properties, to the existing polymers.[1–3] Surface modification of fluoropolymers, for example, poly(vinylidene fluoride) (PVDF), has been of particular interest because the fluoropolymers are one of the most important families of engineering polymers. They are well known for their physical and chemical resistance.[4–6] In addition to numerous and versatile industrial applications, new developments of PVDF have been found in biotechnology,[7–10] and in the biomedical sector (vascular sutures and regeneration templates).[11–13] But the biomedical equipments could be polluted easily because of the low surface energy and hydrophobility of PVDF. To improve surface hydrophilicity of PVDF, a large amount of work had been devoted to the surface modification of fluoropolymers by chemical,[14] plasma,[15–17] irradiation,[18] corona discharge,[19] flame,[20] and ozone treatment.[21] Recently, much attention has been centered on the modification of fluoropolymers via surface graft copolymerization or surface-initiated polymerization.[5,22–28]

Progress in polymerization has made it possible to produce polymer chains or brushes on a surface with controlled length and structure.[1,29] Polymers of various architectures (block, comb, graft, hyperbranched, star, etc.) have been synthesized by living radical polymerizations. Successful examples of the living radical polymerization include nitroxide-mediated radical polymerization,[30] atom transfer radical polymerization (ATRP),[31,32] and reversible addition–fragmentation chain transfer (RAFT) polymerization.[33] ATRP does not require stringent experimental conditions, as in the case of cationic and anionic polymerization. Preparation of well-defined polymer brushes via surface-initiated living radical polymerization has also received a considerable amount of attention in recent years.[34–44]

In the present work, surface modifications of the PVDF film with well-defined polymer brushes from a combination of surface hydroxylation and surface-initiated ATRP are reported. Surface hydroxylation is first generated on the PVDF surface by chemical treatment. The wet chemical treatment is applicable to modify the larger bulky materials, whereas the other traditional treatments are unsuitable. Immobilization

Correspondence to: Y. Chen (ywchen@ncu.edu.cn).
Contract grant sponsor: National Natural Science Foundation of China; contract grant number: 50403016.

of initiators is carried out by esterification of hydroxyl groups covalently linked to the surface and 2-bromoisobutyrate bromide. The tethered 2-bromoisobutyrate is used as the surface-immobilized initiator for ATRP. Homopolymer brushes of methyl methacrylate (MMA) and poly(ethylene glycol) monomethacrylate (PEGMA) are prepared by ATRP on the bromoester-functionalized PVDF surface. Diblock copolymer brushes were prepared by using the homopolymer brushes as the macroinitiators for the ATRP of the second monomer. The chemical composition and hydrophilic property of the nontreated and functionalized PVDF surfaces are determined by X-ray photoelectron spectroscopy (XPS) and contact angle measurement.

EXPERIMENTAL

Materials

PVDF films having a thickness of 0.5 mm were obtained from Goodfellow Cambridge Limited of Huntingon, England. The PVDF films were sliced into rectangular strips of about 1 cm $\times$ 2 cm in size. To remove the organic residues on the surface, the PVDF film was washed with acetone, methanol, and doubly distilled water in the order. The films were dried under reduced pressure at room temperature for about 24 h and then stored in a clean and dry box.

Lithium hydroxide monohydrate (LiOH H_2O, 56%), sodium borohydride ($NaBH_4$, 99%), and diisobutylaluminium hydride (DIBAL-H, 1.0*M* solution in toluene) were purchased from Acros Organics (Geel, Belgium) and used as received. Poly(ethylene glycol) methyl ether monomethacrylate (PEGMA) macromonomer (M_n~300) was passed through the inhibitor remover column to remove the inhibitors. Methyl methacrylate (MMA) and (2-dimethylamino)ethyl methacrylate (DMAEMA) were distilled under reduced pressure and stored in an argon atmosphere at -10°C. Copper(I) bromide and copper(I) chloride were purified according to procedures described in the literature.[45] 2,2-Bipyridine (Bpy), ethyl bromoisobutyrate (EBiB), 2-bromoisobutyrate bromide, 1,1,4,7,10, 10-hexamethyltriethylenetetramine (HMTETA), and other chemical reagents were used without further purification.

Surface characterization

Attenuated total reflectance (ATR) FTIR spectra of the surface-functionalized films were obtained from a Nicolet 5700 FTIR spectrophotometer, using a ZnSe prism with an incident angle of 60°. Each spectrum was collected by cumulating 1024 scans at a resolution of 4 cm^{-1}. A contact angle measurement JC2000A was used to measure static water contact angles of the polymer films at 25°C and 60% relative humidity using a sessile drop method. For each angle reported, at least five sample readings from different surface locations were averaged. The angles reported were reliable to $\pm$ 1°. Gel permeation chromatography (GPC) measurements were carried out using a Waters 1515 HPLC equipped with a Styragel MIXED-C column and a Waters 2414 refractive index detector. THF was used as the mobile phase. Monodispersed polystyrene (PSt) standards (Aldrich Chemical Co.) were used to generate the calibration curve.

The chemical composition of the nontreated and the functionalized PVDF surfaces was determined by X-ray photoelectron spectroscopy (XPS). The XPS measurements were performed on a Kratos AXIS Ultra spectrometer, using a monochromatic Al Kα X-ray source (1486.71 eV photons) at a constant dwell time of 100 ms and a pass energy of 40 eV. The samples were mounted on the standard sample studs by means of double-sided adhesive tapes. The core-level signals were obtained at a photoelectron takeoff angle (α, measured with respect to the sample surface) of 90°. The X-ray source was run at a reduced power of 225 W (15 kV and 15 mA). The pressure in the analysis chamber was maintained at 10^{-8} Torr or lower during each measurement. All binding energies (BE's) were referenced to the C 1s hydrocarbon peak at 284.8 eV. Surface elemental stoichiometries were determined from the spectral area ratios, after correcting with the experimentally determined sensitivity factors, and were reliable to within $\pm$ 10%. The elemental sensitivity factors were calibrated using stable binary compounds of well-established stoichiometries.

The thickness of the polymer films grafted on the PVDF substrates was determined by ellipsometry. The measurements were carried out on a variable angle spectroscopic ellipsometer (M-2000, J. A. Woollam Inc., Lincoln, NE) at incident angles of 60° and 65° in the wavelength range 370–1000 nm. The refractive index of the dried films at all wavelengths was assumed to be 1.5. All measurements were conducted in the dry air at room temperature. For each sample, thickness measurements were made on at least three different surface locations. Each thickness reported was reliable to $\pm$ 1 nm. Data were recorded and processed using the WVASE32 software package.

Surface hydroxylation of PVDF film

The surface hydroxylation of PVDF films was carried out by treatment of PVDF films with aqueous LiOH, followed by successive reductions with $NaBH_4$ and DIBAL-H, according to the literature.[46] The PVDF film was immersed into a solution of 1.8 mol/L LiOH H_2O in water. The solution was maintained at 80°C and stirred. After 24 h of reaction, the sample was detached and rinsed successively with water and 2-propanol. The film was dried under vacuum. The film

sample, previously treated with LiOH, was immersed into a solution of 0.078 mol/L $NaBH_4$ in 2-propanol. The solution was maintained at 20°C and stirred. After 17 h of reaction, the sample was detached and rinsed successively with 2-propanol, a 1 : 1 (v/v) mixture of 1*N* HCl and ethanol, and a 1 : 1 (v/v) mixture of acetone and water. The film was dried under vacuum. Subsequently, the film sample previously treated with LiOH and $NaBH_4$ was immersed into a 0.104 mol/L of DIBAL-H/toluene solution. After 65 h of reaction at room temperature, the sample was rinsed successively with hexane, a 1 : 1 (v/v) mixture of 1*N* HCl and ethanol, and a 1 : 1 (v/v) mixture of acetone and water.

Immobilization of the initiator on the hydroxylated PVDF surface

To a solution of 3 mL of pyridine in 100 mL dry diethyl ether was added 9 pieces of the hydroxylated PVDF substrates, followed by dropwise addition of 4 mL of 2-bromoisobutyrate bromide in 60 mL of dry diethyl ether over 10 min. The reaction mixture was gently stirred at 0°C for 2 h, and then at room temperature for another 10 h. The so-modified PVDF substrates (PVDF-Br) were removed and washed with ethanol and doubly distilled water. The substrates were then dried by pumping under reduced pressure for about 10 h.

Surface initiated atom transfer radical polymerization

For the preparation of poly(methyl methacrylate) (PMMA) brushes on the PVDF-Br surface, MMA (2 mL, 18.6 mmol), CuBr (9 mg, 0.062 mmol), and HMTETA (51 μL, 0.186 mmol) were added to 2 mL of a mixed solvent (anisole:acetonitrile, 1 : 1, v/v). The solution was degassed with argon for 20 min. The PVDF-Br substrate and the free initiator, EBiB (9 μL, 0.062 mmol), were then added to the solution. The reaction flask was sealed and kept in a 70°C oil bath for a predetermined period of time. After the reaction, the PVDF substrate with surface-grafted PMMA (the PVDF-*g*-PMMA surface) was removed from the solution and extracted thoroughly with excess acetone for 48 h. The "free" PMMA formed in solution by the free initiator was recovered by precipitating in excess methanol. Monomer conversion was determined gravimetrically.

For the preparation of poly(ethylene glycol) monomethacrylate) (PPEGMA) brushes on the PVDF-Br surface, PEGMA (2.5 mL, 7.5 mmol), CuCl (7.5 mg, 0.075 mmol), $CuCl_2$ (2 mg, 0.015 mmol), and Bpy (28 mg, 0.18 mmol) were added to 2 mL of doubly distilled water. The mixture was stirred and purged with argon for 30 min. The PVDF-Br substrate was then introduced into the solution. The reaction flask was sealed and placed in a 25°C water bath for a predetermined period of time. After the reaction, the PVDF substrate with surface-grafted PPEGMA (the PVDF-*g*-PPEGMA surface) was removed from the reaction mixture and extracted thoroughly with excess ethanol over 10 h.

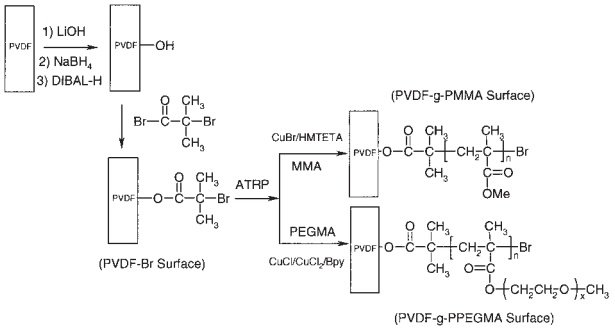

Figure 1 Schematic diagram illustrating the processes of hydroxylation of PVDF surface, formation of the 2-bromoisobutyrate-functionalized PVDF surface, and surface graft polymerization via ATRP from the bromoester-flinctionalized PVDF surface.

For the preparation of poly((2-dimethylamino)ethyl methacrylate) (PDMAEMA) block on the PVDF-*g*-PMMA and PVDF-*g*-PPEGMA surfaces, DMAEMA (3.3 mL, 20 mmol), CuBr (14.4 mg, 0.1 mmol), and HMTETA (81.6 μL, 0.3 mmol) were added to 3 mL of a mixed solvent (anisole: acetonitrile, 1 : 1, v/v). The solution was degassed with argon for 30 min. The PVDF-*g*-PMMA (or PVDF-*g*-PPEGMA) substrate, instead of PVDF-Br substrate, and the free initiator, EBiB (14.4 μL, 0.1 mmol), were added to the solution. The reaction flask was sealed and placed in a 60°C oil bath for 12 h. After the reaction, the PVDF substrate with surface-grafted PMMA-*b*-PDMAEMA (or PPEGMA-*b*-PDMAEMA) copolymer brushes (the PVDF-*g*-PMMA-*b*-PDMAEMA or PVDF-*g*-PPEGMA-*b*-PDMAEMA substrate) was removed from the solution and washed thoroughly with excess acetone, ethanol, and doubly distilled water to remove any adhered monomer and homopolymer.

RESULTS AND DISCUSSION

Surface hydroxylation of PVDF films

The surface of PVDF film was selectively modified by wet chemistry according to the procedures (Fig. 1).[46] Treatment with aqueous LiOH produced HF elimination and the emergence of an oxygen-containing functionality. The dehydrofluorination of PVDF films was performed with aqueous lithium hydroxide solution at 80°C. No color change was observed. Examination of the treated samples by optical microscopy did not show cracks or other surface defects. The results indi-

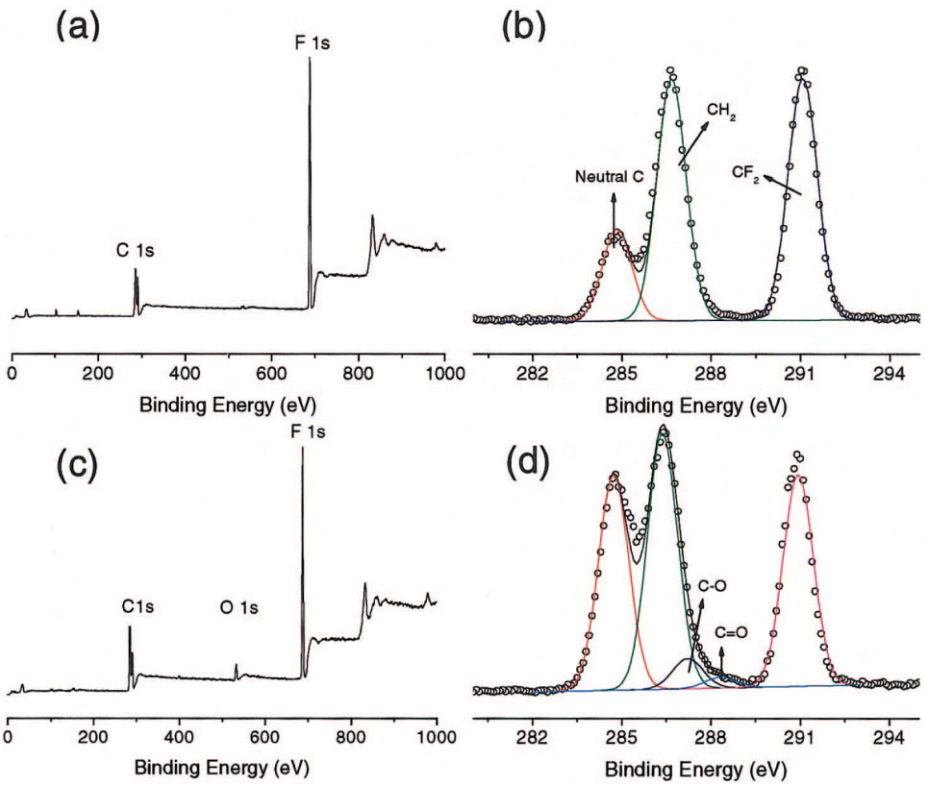

Figure 2 XPS wide-scan spectra of (a) the nontreated PVDF surface and (c) the hydroxylated PVDF surface, and C 1s core-level spectra of (b) the nontreated PVDF surface, and (d) the hydroxylated PVDF surface. [Color figure can be viewed in the online issue, which is available at www.interscience.wiley.com.]

cated the presence of ketone-, ether (epoxide)-, and alcohol motifs. It gave rise to the increase of surface hydrophilicity of the PVDF films treated with LiOH–H_2O from 93 to 63°. The percentage of alcohols could be significantly increased by reduction of the ketones with $NaBH_4$ in 2-propanol, followed by reduction of the epoxides with DIBAL-H in toluene. The PVDF films, initially treated with LiOH, were immersed into a solution of $NaBH_4$ in 2-propanol, followed by a solution of DIBAL-H in toluene. After neutralization, rinsing, and drying, the sample surfaces were characterized by the contact angle of water. An unexpected diminution of the hydrophilic character was observed. The static contact angle of the PVDF film treated with $NaBH_4$ and DIBAL-H increased to 80° and 83°, respectively, even though still lower than that of the nontreated PVDF film. The literature also reflected the similar tendence.[46] The wide-scan and C 1s core-level spectra of the nontreated PVDF film and the hydroxylated PVDF film are shown in Figures 2(a–d), respectively. For the nontreated PVDF surface, the wide-scan spectrum comprises, predominately, two peaks at the BEs of about 286 and 688 eV, attributable to the C 1s and F 1s signals, while the wide-scan spectrum of the hydroxylated PVDF surface comprises not only C 1s and F 1s but also O 1s signal. A [O]/[F] ratio of about 0.13 was obtained from O 1s and F 1s spectral area. The C 1s core-level spectrum of the nontreated PVDF surface consists of two peak components of about equal integral area with BE at 286.4 eV for the CH_2 species and at 290.9 eV for the CF_2 species. There is a substantial peak component at 284.6 eV, attributable to neutral carbon, which might be the result of organic contamination on the surface. Hydroxylation treatment causes the breakage of C—F bonds, resulting in formation of C—OH of the PVDF surface. Surface hydroxylation was also ascertained by the appearance of two new peak components at the BEs of about 286.6 and 288.1 eV, attributable to the C—O and C═O species, in the C 1s core-level spectrum of the hydroxylated PVDF surface. The presence of a trace amount of the C═O species was arisen from incomplete reduction by $NaBH_4$ treatment.

The hydroxyl coverage on the treated PVDF films was further estimated by radiolabeling experiments. Small samples were immersed into a mixture of [^{3}H]-acetic anhydride and pyridine in toluene (1 h, 20°C), a reactive medium that could selectively derivatize the alcohols into acetates, without affecting the other oxygen-containing functions (ketone, epoxide). After appropriate washings for removing most of the unreacted [^{3}H]-acetic anhydride, the radioactivity associated to the samples was determined by liquid scintillation counting (LSC). The measured radioactiv-

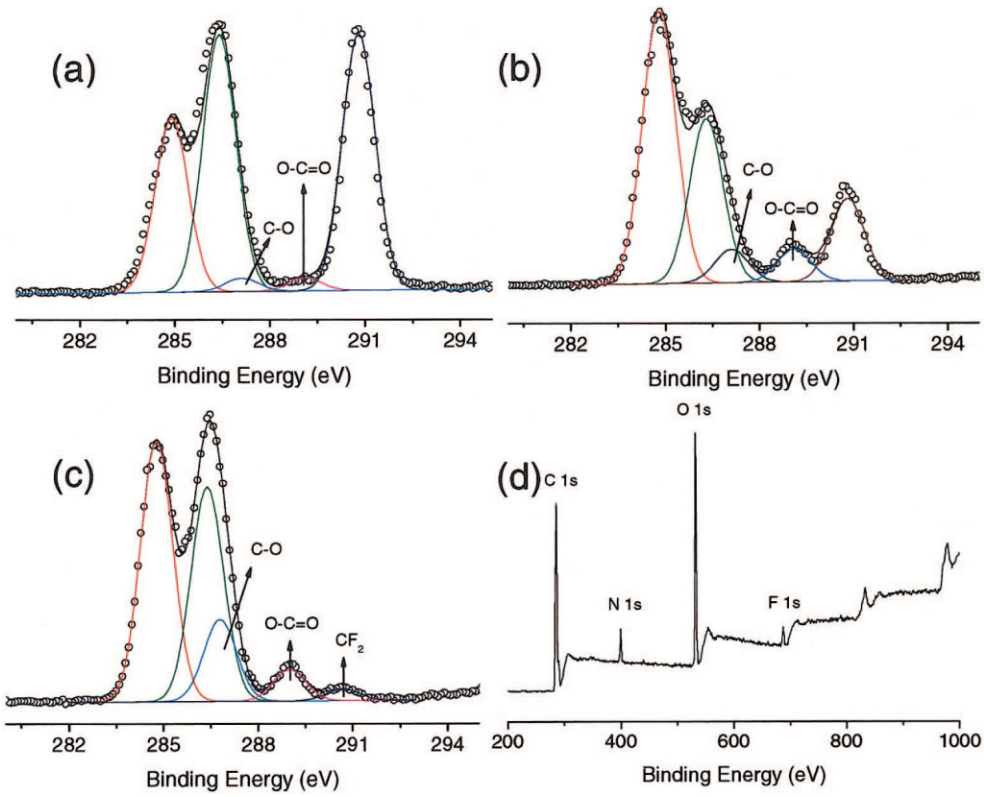

Figure 3 XPS C 1s core-level spectra of (a) the PVDF-Br surface, (b) the PVDF-*g*-PMMA surface from 1 h of surface-initiated ATRP, (c) the PVDF-*g*-PPEGMA surface from 5 h of surface-initiated ATRP, and (d) wide-scan spectrum of PVDF-*g*-PPEGMA-b-PDMAEMA surface. [Color figure can be viewed in the online issue, which is available at www.interscience.wiley.com.]

ity could be correlated with the amount of fixed label. Nevertheless, some irreversible adsorption, or diffusion, of the radioactive label into the polymer interface could not be excluded. This contribution of nonspecific fixation of [^{3}H]-acetic anhydride was estimated by the counting (LSC) of a blank sample. Subtraction of this nonspecific contribution from the experimental counting values gave the accurate reactivity assays of the hydroxyl functions covalently linked to the surface. The experimental radioactivity was converted to hydroxyl units per surface area (nm^2). About 0.4 units/nm^2 of the hydroxyl coverage on the treated PVDF surface was obtained.

Immobilization of the initiator on the hydroxylated PVDF surface

To prepare the polymer brush on the PVDF surface, a uniform and dense layer of initiators immobilized on the PVDF surface is indispensable. Coupling of the α-bromoester group-terminated monolayers to the PVDF surface was performed using the well-established esterification of the hydroxyl groups covalently linked to the surface with 2-bromoisobutyrate bromide. The presence of the absorption band at 1710 cm^{-1}, attributable to the stretching of the ester carbonyl group, in the ATR FTIR spectrum of the PVDF-Br substrate indicated that the 2-bromoisobutyrate species has been successfully immobilized on the PVDF surface. After immobilization of the 2-bromoisobutyrate segments, the static contact angle of the PVDF-Br surface was measured to be 90°, due to the presence of halide. The presence of the Br 3 days core-level spectrum at the BE of around 70.5 eV and the appearance of the O—C═O peak component in the C 1s core-level spectrum of the 2-bromoisobutyrate-functionalized PVDF surface indicated that the 2-bromoisobutyrate species has been successfully immobilized on the PVDF surface. The C 1s core-level spectrum of the PVDF-Br surface is shown in Figure 3(a). Fairly good agreement between the XPS-derived and theoretical [C—O] : [O—C═O] ratio is observed for the 2-bromoisobutyrate-functionalized PVDF surface. The initiator concentration on the PVDF surface can be defined simply as the [Br]/[F] ratio and can be derived from the Br 3 days and F 1s spectral area. An initiator concentration of about 0.09 is obtained for the PVDF-Br surface. The persistence of very strong F signals in the wide scan spectrum of the PVDF-Br surface provides additional evidence to the fact that the thickness of monolayer is much less than the sam-

pling depth of the XPS technique (about 7.5 nm in an organic matrix). Because of the probing depth of XPS technique, an initiator concentration of about 0.09, as defined by [Br]/[F] ratio, should be less than actual values. The radiolabeling experiments revealed that all hydroxyl groups were consumed to immobilize the initiator groups. Therefore, the initiator coverage on the PVDF-Br surface was regarded as 0.4 units/nm^2.

Surface initiated polymerization from the α-bromoester-functionalized PVDF surface via ATRP

The advantage of ATRP over other living polymerization, such as anionic and cationic polymerization, is the tolerance for various functionalities in the monomers, leading to polymers with functionalities along the chains. Therefore, the physicochemical properties of the PVDF surface can be tuned by the choice of a variety of vinyl monomers. In addition to the selection of MMA as the model monomer, an additional functional monomer, PEGMA, is also selected. The PEGMA polymer-grafted PVDF surface could be effective in preventing protein adsorption and platelet adhesion. A biocompatible PVDF surface prepared from PEGMA graft polymerization can be used in the PVDF-based biomedical microdevices.

A sufficient concentration of the deactivating Cu(II) complex is necessary to rapidly establish an equilibrium between the dormant and the active chains at the begin of ATRP. In the absence of this controlled equilibrium, the process resembles that of the conventional redox-initiated radical polymerization.[31] The Cu(II) species can be obtained by the reaction of Cu(I) complex with the initiator to produce the active radical for propagation, or by addition at the beginning of reaction. The main difference between ATRP from a surface and ATRP in bulk or solution is the relatively low concentration of the initiator immobilized on the surface. The low surface initiator concentration can lead to a low concentration of the deactivating species (Cu(II) complex) being formed at the beginning of polymerization. The problem can be resolved by two approaches. One is the addition of the free initiator at the begin of reaction, and the other is the addition of the deactivator (Cu(II) complex). Because of the difficulty in obtaining the molecular weight of the grafted polymer on the PVDF surface, the first approach was chosen to control the ATRP from the surface. In addition, the "free" polymer formed by the free initiator in solution can be used to monitor the properties of the grafted polymer. Thus, the free initiator serves not only as a mediator for ATRP on the surface, but also as an indicator of surface graft polymerization.

Initial experiments using anisole as solvent for ATRP from the PVDF-Br surface did not yield good results. Copper precipitation on the flask wall was observed at high conversion. Previous studies have shown that the use of polar solvents for ATRP can result in an increase in polymerization rate and dissolution of the copper complex.[31] Thus, a mixed solvent (anisole:acetonitrile = 1 : 1, v/v) was chosen for carrying out the ATRP of MMA on the PVDF-Br surface. No copper precipitation was observed during ATRP. The reaction medium remains homogeneous throughout the polymerization process.

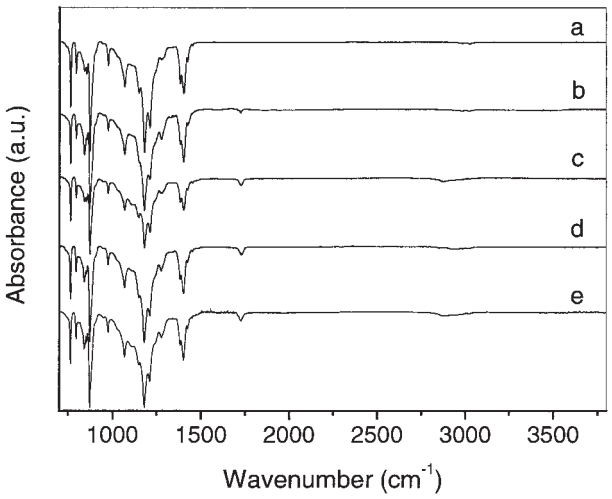

Figure 4 ATR–FTIR spectra of (a) the nontreated PVDF surface, and the PVDF-Br surface subjected to ATRP of MMA for (b) 0.5 h, (c) 1 h, (d) 10 h, and (e) 17 h. Reaction conditions: [MMA] : [EBiB] : [CuBr] : [HMTETA] = 300 : 1 : 1 : 3, [MMA] = 4.7*M*, solvent anisole/acetonitrile = 1/1 (v/v), temp. 70°C.

The presence of grafted polymer on the PVDF surface is ascertained first by ATR–FTIR spectra. The ATR–FTIR spectra of the PVDF-*g*-PMMA and the PVDF-*g*-PPEGMA surface reveal the appearance of the absorption band at 1730 cm^{-1}, attributable to the stretching of ester carbonyl group, as shown in Figures 4 and 5, respectively. The variations in graft concentration are reflected in the changes in ratio of the intensity of the absorption band at 1730 cm^{-1} to that of the absorption band at 1400 cm^{-1}.

The presence of grafted polymer on the PVDF surface is ascertained by XPS analysis. The results are shown in Figure 3. The C 1s core-level spectra of the PVDF-*g*-PMMA surface (part b) and PVDF-*g*-PPPEGMA surface (part c) can be curve-fitted with five peak components having BE's at about 284.8, 286.2, 286.6, 288.9, and 290.9 eV, attributable to the C—H, CH_2, C—O, O—C═O, and CF_2 species, respectively. The [C—O] : [O—C═O] ratios of the PVDF-*g*-PMMA and PVDF-*g*-PPPEGMA surface, obtained from XPS analysis, are in fairly good agreement with the respective theoretical ratios. In addition, the CF_2 peak component associated with the PVDF substrate persists in the curve-fitted C 1s core-level spectra of the PVDF-*g*-PMMA and PVDF-*g*-PPPEGMA surface,

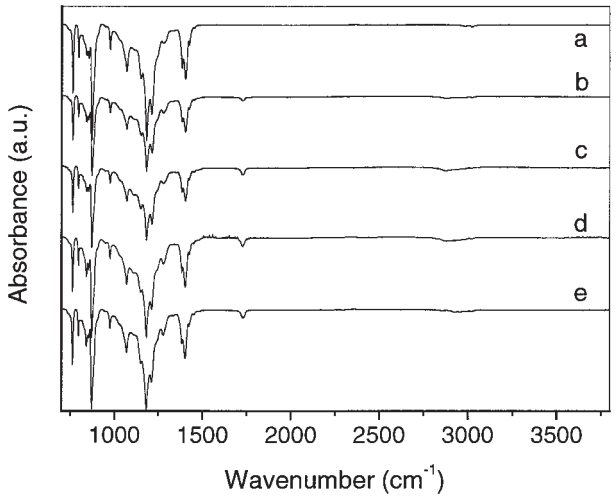

Figure 5 ATR–FTIR spectra of (a) the nontreated PVDF surface, and the PVDF-Br surface subjected to ATRP of PEGMA for (b) 1 h, (c) 5 h, (d) 17 h, and (e) 22 h. Reaction conditions: [PEGMA] : [CuCl] : [$CuCl_2$] : [Bpy] = 100 : 1 : 0.2 : 2.4, [PEGMA] = 1.8*M*, solvent water, temp. 25°C.

but presents a lower area in comparison to the CH_2 component. The graft concentration of the PMMA and PPEGMA brushes grown on the PVDF surface can be derived from the O—C═O peak component to the CF_2 peak component. With the increase of graft polymerization time, the [O—C═O] : [CF_2] ratio increases for both graft-functionalized PVDF surfaces, until CF_2 peak component cannot be determined by XPS. This result suggests that thickness of the grafted polymer layer is gained gradually until thickness of graft layer is beyond the probing depth of the XPS technique.

The variation in water contact angle for the PVDF surfaces with different polymer brushes indicates that the hydrophilicity of the PVDF surface can be easily tuned. The contact angle of the nontreated PVDF surface is about 93°. As shown in Table I, the PVDF surface with a PMMA graft layer has a contact angle of about 84°. As presented in Figure 6, when grafted with a PPEGMA layer, the PVDF surface becomes more hydrophilic and the contact angle decreases with increase of graft concentration (relative to reaction time).

The ellipsometry measurements indicate a large increase in film thickness after the growth of the PMMA and PPEGMA layer on the PVDF surface. The results confirm that the increase in thickness observed is the result of graft polymerization from the 2-bromoisobutyrate-functionalized PVDF surface. Furthermore, because ATRP is a "living" polymerization process, the thickness of the polymer brushes should increase linearly with the polymerization time and the molecular weight of the graft polymer. As shown in Figure 7, an approximately linear increase in thickness of the grafted PMMA and PPEGMA layer on the PVDF-Br surface with the polymerization time is observed. A

TABLE I
Water Contact Angle of the Functionalized-PVDF Surfaces

Sample	Contact angle (°)	Film thickness (nm)
PVDF-*g*-PMMA[a]	84	7.9
PVDF-*g*-PPEGMA[b]	58	8.6
PVDF-*g*-PMMA-*b*-PDMAEMA[c]	56	14.5
PVDF-*g*-PPEGMA-*b*-PDMAEMA[d]	61	17.0

[a] Reaction conditions: [MMA] : [EBiB] : [CuBr] : [HMTETA] = 300 : 1 : 1 : 3, [MMA] = 4.7*M*, solvent anisole/acetonitrile = 1/1 (v/v), temp 70°C, reaction time 5 h.

[b] Reaction conditions: [PEGMA] : [CuCl] : [$CuCl_2$] : [Bpy] = 100 : 1 : 0.2 : 2.4, [PEGMA] = 1.8*M*, solvent water, temp. 25°C, reaction time 5 h.

[c] Prepared from ATRP of DMAEMA subjected to PVDF-*g*-PMMA, obtained from ATRP of MMA for 5 h. Reaction conditions: [DMAEMA] : [CuBr] : [HMTETA] : [EBiB] = 200 : 1 : 3 : 1, [DMAEMA] = 3*M*, solvent anisole/acetonitrile = 1/1 (v/v), temp. 60°C, reaction time 12 h.

[d] Prepared from ATRP of DMAEMA subjected to PVDF-*g*-PPEGMA, obtained from ATRP of PEGMA for 5 h. Reaction conditions: [DMAEMA] : [CuBr] : [HMTETA] : [EBiB] = 200 : 1 : 3 : 1, [DMAEMA] = 3*M*, solvent anisole/acetonitrile = 1/1 (v/v), temp 60°C, reaction time 12 h.

linear relationship between the thickness of the PMMA layer and the molecular weight of the "free" PMMA formed in the solution is also observed (inserted figure). These results indicate that the process of surface-initiated ATRP of MMA and PEGMA is controlled.

Additional evidence on the controlled polymerization is also obtained from the "free" PMMA formed by the free initiator. Figure 8(a) shows the linearity relationship between ln([M_0]/[M]) and time, where [M_0] is the initial monomer concentration and [M] is the

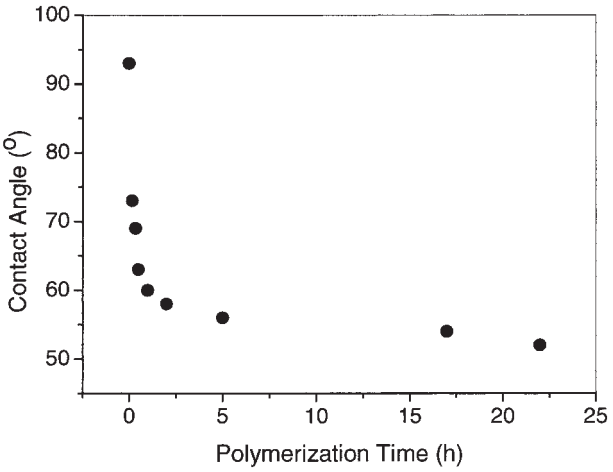

Figure 6 The water contact angles of the PVDF-*g*-PPEGMA surface from different graft polymerization time of surface-initiated ATRP.

monomer concentration. The result indicates that the concentration of the growing species remains constant and a first-order kinetic is obtained. Figure 8(b) shows the relationship between M_n of the free PMMA and the conversion of the MMA monomer. The number–average molecular weight of the "free" PMMA increases linearly with the increase in monomer conversion. The polydispersity index (M_w/M_n) of the free PMMA is also around 1.2. Although the exact molecular weight of the polymer grafted on the PVDF surface is not known, the molecular weight of the grafted polymer is expected to be proportional to that of the polymer formed in the solution.[34,43] These results indicate that the processes of the surface-initiated ATRP of MMA and PEGMA are controlled.

Block copolymer brushes

Another advantage of ATRP over the conventional radical polymerization technique is the possibility for the synthesis of block copolymers. ATRP is used to synthesize the PMMA-*b*-PDMAEMA and PPEGMA-*b*-PDMAEMA diblock copolymer brushes from the α-bromoester-functionalized PVDF surface. The formation of block copolymer brushes was confirmed by the XPS, contact angle, and ellipsometry. A 8.4 nm increase in the thickness of the grafted polymer layer was observed by ellipsometry after ATRP of DMAEMA at 60°C for 12 h on the PVDF-*g*-PPEGMA surface (initial thickness 8.6 nm), whereas a 6.6 nm increase in the thickness of the grafted polymer layer was observed after ATRP of DMAEMA at 60°C for 12 h on the PVDF-*g*-PMMA surface (initial thickness 7.9 nm). Significant increases in surface coverage of the grafted polymer brushes were observed after ATRP of DMAEMA on the PVDF-*g*-PMMA and PVDF-*g*-PPEGMA surfaces. A new N 1s peak component at the BE of 398.5 eV has appeared in the XPS wide-scan spectrum of the PVDF-*g*-PPEGMA-*b*-PDMAEMA surface [Fig. 3(d)]. These results confirm that some of the dormant sites at the ends of the grafted PPEGMA and PMMA chains allow the reactivation of the graft polymerization process, resulting in the forma-

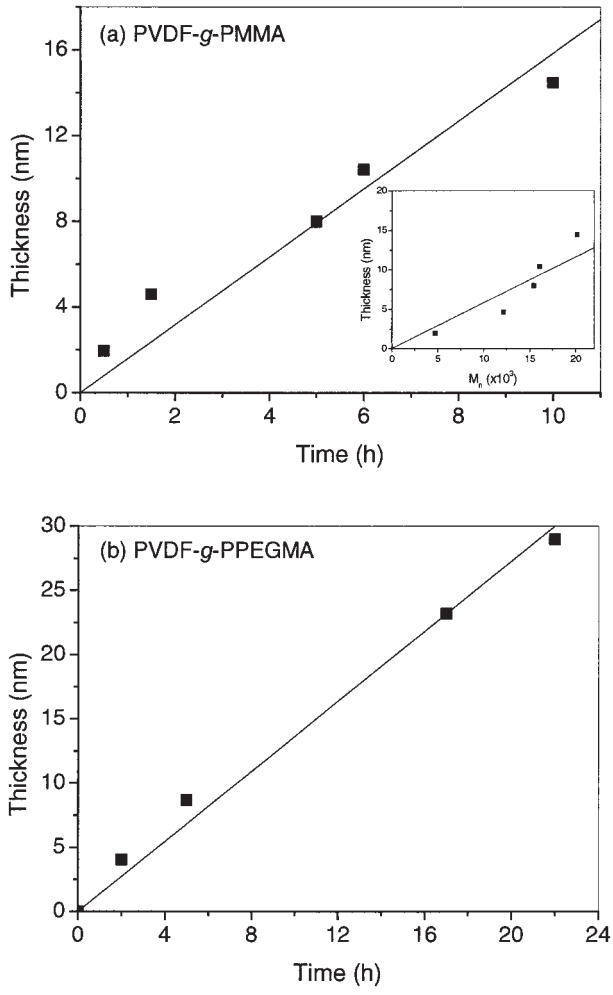

Figure 7 Dependence of the thickness of (a) the PMMA layer and (b) the PPEGMA layer, grown from the PVDF-Br surface via ATRP, on polymerization time; Insert: Dependence of the thickness of the PMMA layer on molecular weight (M_n) of the "free" PMMA formed in the solution.

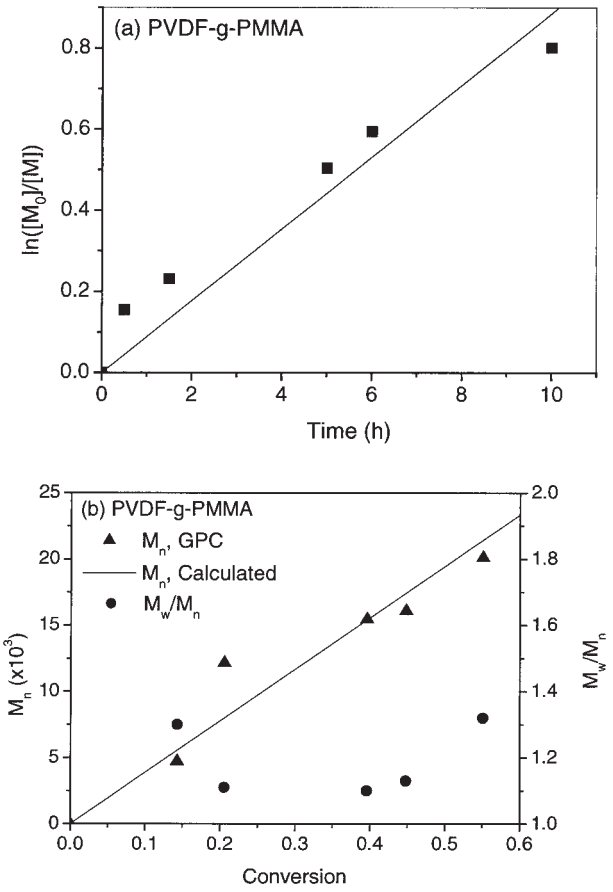

Figure 8 The relationship (a) between ln([M_0]/[M]) and polymerization time and (b) between M_n and monomer conversion. Reaction conditions: [MMA] : [EBiB] : [CuBr] : [HMTETA) = 300 : 1 : 1 : 3, [MMA] = 4.7*M*, solvent anisole/acetonitrile = 1/1 (v/v), temp. 70°C.

tion of the block copolymer brushes on the PVDF surface. The C—N peak component arises solely from the PDMAEMA block of the PPEGMA-*b*-PDMAEMA copolymer brush. The water contact angles of the diblock polymer brushes on the PVDF surfaces are also shown in Table I. After DMAEMA has been block-copolymerized onto the PMMA brushes, the contact angle of the PVDF-*g*-PMMA-*b*-PDMAEMA surface decreases from 84 to 56°, whereas the contact angle of the PVDF-*g*-PPEGMA-*b*-PDMAEMA surface increases from about 58 to 61° after DMAEMA has been block-copolymerized onto the PPEGMA brushes. The contact angles are comparable to that of the homopolymer brushes of PDMAEMA on the PVDF surface.

CONCLUSIONS

Controlled grafting of well-defined polymer brushes of PMMA and PPEGMA was carried out via ATRP on the PVDF surfaces. Prior to the surface-initiated ATRP, the PVDF surface was hydroxylated in three steps: treatment with LiOH, reduction with $NaBH_4$, and reduction with DIBAL-H. The immobilization of initiator was performed by esterification of the hydroxyl groups covalently linked to the surface with 2-bromoisobutyrate bromide. ATR–FTIR and contact angle data indicated the formation of polymer brushes on the PVDF surface. Kinetics studies revealed a linear increase in surface coverage of the surface graft polymer brushes with reaction time, indicating that the chain growth from the surface was a controlled process with "living" characteristics. Diblock copolymer brushes consisting of PMMA or PPEGMA and PDMAEMA blocks were obtained on the PVDF surfaces, using either type of the homopolymer brushes as the macroinitiators for ATRP of the second monomer. The homopolymer and block copolymer covalently tethered to the PVDF surface have imparted new and well-structured functionalities directly onto the fluoropolymer surfaces.

The author thanks the Analytic center of Nanchang University for providing analytic finance.

References

1. Zhao, B.; Brittain, W. J. Prog Polym Sci 2000, 25, 667.
2. Kato, K.; Uchida, E.; Kang, E. T.; Uyama, Y.; Ikada, Y. Prog Polym Sci 2003, 28, 209.
3. Uyama, Y.; Kato, K.; Ikada, Y. Adv Polym Sci 1998, 137, 1.
4. Souzy, R.; Ameduri, B.; Boutevin, B. Prog Polym Sci 2004, 29, 75.
5. Kang, E. T.; Zhang, Y. Adv Mater 2000, 12, 1481.
6. Sacher, E. Prog Surf Sci 1994, 47, 273.
7. Pereira Nunes, S.; Peinemann, K. V. J Membr Sci 1992, 73, 25.
8. Flösch, D.; Lehmann, H.-D.; Reichl, R.; Inacker, O.; Göpel, W. J Membr Sci 1992, 70, 53.
9. Vestling, M. M.; Fenselau, C. Biochem Soc Trans 1994, 22, 547.
10. Speicher, D. W. Methods Enzymol 1994, 6, 262.
11. Urban, E.; King, M. W.; Guidon, R.; Laroche, G.; Marois, Y.; Martin, L.; Cardou, A.; Douville, Y. ASAIO J 1994, 40, 145.
12. Laroche, G.; Marois, Y.; Guidon, R.; King, M. W.; Martin, L.; How, T.; Douville, Y. J Biomed Mater Res 1995, 29, 1525.
13. Valentini, R. F.; Vargo, T. G.; Gardella, J. A., Jr.; Aebischer, P. J Biomater Sci Polym Ed 1993, 5, 13.
14. Costello, C. A.; McCarthy, T. J. Macromolecules 1987, 20, 2819.
15. Chan, C. M.; Ko, T. M.; Hiraoka, H. Surf Sci Rep 1996, 24, 1.
16. Griesser, H. J.; Da, Y.; Hughes, A. E.; Gengenbach, T. R.; Mau, A. W. H. Langmuir 1991, 7, 2484.
17. Golub, M. A.; Lopata, F. S.; Finney, L. S. Langmuir 1994, 10, 3629.
18. Tian, J.; Xue, Q. J. J Appl Polym Sci 1998, 69, 435.
19. Vasilets, V. N.; Hirata, I.; Iwata, H.; Ikada, Y. J Polym Sci Polym Chem 1998, 36, 2215.
20. Mathieson, I.; Brewis, D. M.; Sutherland, I.; Cayless, R. A. J Adhes 1994, 46, 49.
21. Boutevin, B.; Robin, J. J.; Serdani, A. Eur Polym J 1992, 28, 1507.
22. Tan, K. L.; Woon, L. L.; Wong, H. K.; Kang, E. T.; Neoh, K. G. Macromolecules 1993, 26, 2832.
23. Inagaki, N.; Tasaka, S.; Goto, Y. J Appl Polym Sci 1997, 66, 77.
24. Yang, M. R.; Chen, K. S. Mater Chem Phys 1997, 50, 11.
25. Becker, W.; Bothe, M.; Schmidt-Naake, G. Angew Makromol Chem 1999, 273, 57.
26. Akinay, E.; Tincer, T. J Appl Polym Sci 2001, 79, 816.
27. Konig, U.; Nitschke, M.; Menning, A.; Eberth, G.; Pilz, M.; Arnhold, C.; Simon, F.; Adam, G.; Werner, C. Colloids Surf B 2002, 24, 63.
28. Li, J. Y.; Sato, K.; Ichiduri, S.; Asano, S.; Ikeda, S.; Iida, M.; Oshima, A.; Tabata, Y.; Washio, M. Eur Polym J 2004, 40, 775.
29. Edmondson, S.; Osborne, V. L.; Huck, W. T. S. Chem Soc Rev 2004, 33, 14.
30. Hawker, C. J.; Bosman, A. W.; Harth, E. Chem Rev 2001, 101, 3661.
31. Matyjaszewski, K.; Xia, J. Chem Rev 2001, 101, 2921.
32. Kamigaito, M.; Ando, T.; Sawamoto, M. Chem Rev 2001, 101, 3689.
33. Chiefari, J.; Chong, Y. K.; Ercole, F.; Krstina, J.; Jeffery, J.; Le, T. P. T.; Mayadunne, R. T. A.; Meijs, G. F.; Moad, C. L.; Moad, G.; Rizzardo, E.; Thang, S. H. Macromolecules 1998, 31, 5559.
34. Ejaz, M.; Yamamoto, S.; Ohno, K.; Tsujii, Y.; Fukuda, T. Macromolecules 1998, 31, 5934.
35. Husseman, M.; Malmström, E. E.; McNamara, M.; Mate, M.; Mecerreyes, D.; Benoit, D. G.; Hedrick, J. L.; Mansky, P.; Huang, E.; Russell, T. P.; Hawker, C. J. Macromolecules 1999, 32, 1424.
36. Matyjaszewski, K.; Miller, P. J.; Shukla, N.; Immaraporn, B.; Gelman, A.; Luokala, B. B.; Siclovan, T. M.; Kickelbick, G.; Vallant, T.; Hoffmann, H.; Pakula, T. Macromolecules 1999, 32, 8716.
37. Mori, H.; Boker, A.; Krausch, G.; Müller, A. H. E. Macromolecules 2001, 34, 6874.
38. Tsujii, Y.; Ejaz, M.; Sato, K.; Goto, A.; Fukuda, T. Macromolecules 2001, 34, 8872.
39. Baum, M.; Brittain, W. J. Macromolecules 2002, 35, 610.
40. Zheng, G. D.; Stöver, H. D. H. Macromolecules 2003, 36, 1808.
41. Edmondson, S.; Huck, W. T. S. J Mater Chem 2004, 14, 730.
42. Granville, A. M.; Boyes, S. G.; Akgun, B.; Foster, M. D.; Brittain, W. J. Macromolecules 2004, 37, 2790.
43. Yu, W. H.; Kang, E. T.; Neoh, K. G.; Zhu, S. J Phys Chem B 2003, 107, 10198.
44. Khan, M.; Huck, W. T. S. Macromolecules 2003, 36, 5088.
45. Matyjaszewski, K.; Miller, P. J.; Shukla, N.; Immaraporn, B.; Gelman, A.; Luokala, B. B.; Siclovan, T. M.; Kickelbick, G.; Vallant, T.; Hoffman, H.; Pakula, T. Macromolecules 1999, 32, 8716.
46. Marchand-Brynaert, J.; Jongen, N.; Dewez, J.-L. J Polym Sci Polym Chem 1997, 35, 1227.